Advances in Environmental Technology 11(1) 2025, 13-35.

Iranian Reasearch Organization for Science and Technology (IROST)

Advances in Environmental Technology

Journal home page: https://aet.irost.ir

Investigating the removal of Mn(II) from water and wastewater using low-cost bio-sorbents: orange peels and sugarcane bagasse

Vincent Masilela, Beauclair Nguegang, Abayneh Ataro Ambushe*

Department of Chemical Sciences, Faculty of Science, University of Johannesburg, P.O. Box 524, Auckland Park 2006, Johannesburg, South Africa.

ARTICLE INFO

Document Type:
Research Paper

Article history:
Received 22 February 2024
Received in revised form
16 October 2024
Accepted 19 October 2024

Keywords:
Bio-Sorbents
Manganese
Orange Peels
Sugarcane Bagasse
Water

ABSTRACT

The high content of manganese (Mn) in potable water is a significant public health problem; therefore, it is necessary to lower it to an acceptable level that is mandated by regulatory agencies. This study was motivated by the need to evaluate the efficacy of low-cost and reusable bio-sorbents, namely orange peels (OPs) and sugarcane bagasse (SCB), for the attenuation of Mn(II) from simulated and real effluent. The solid:liquid ratio of 30 mg:100 mL was applied, and the results revealed that OPs removed 96.71% of Mn(II) at an optimum contact period of 120 min while SCB removed 94.74% of Mn(II) at an ideal contact period of 30 min. The pH study revealed the ideal removal efficiency (RE) at pH 5 for both OPs and SCB, while the optimum dosage was 100 mg for OPs and 50 mg for SCB. The study also found that SCB and OPs can be reused up to the third adsorption-desorption cycle without their RE changing significantly in those adsorption-desorption cycles. The bio-sorbents were characterized using Fourier-transform infrared (FTIR) spectroscopy, scanning electron microscopy (SEM) hyphenated to energy-dispersive X-ray spectroscopy (EDS), powder X-ray diffraction (PXRD), zeta potential analyzer, and thermogravimetric analysis (TGA). The characterization results revealed a noticeable difference between pure and water-reacted bio-sorbents. From the findings of this study, the use of OPs and SCB could yield the desired result in Mn(II) removal from water.

1. Introduction

At the forefront of promoting sustainable development, freshwater is crucial in sustaining life on earth and fostering socioeconomic progress while maintaining robust ecosystems. However, the available water resources are under severe threat due to climate change, urbanization, and anthropogenic activities, which release diverse pollutants, including potentially toxic elements (PTEs), to surface and groundwater [1]. Surface and groundwater contaminated by PTEs become toxic to humans and other living organisms, affecting water suitability for myriads of defined use. Amongst the PTEs, Mn is the most abundant in terrestrial and coastal ecosystems, thus increasing its ability to pollute water resources, as reported by Kasim et al. [2]. Specifically, Mn is among the most common contaminants found in

*Corresponding author Tel.: +27 115592329
E-mail: aambushe@uj.ac.za
DOI: 10.22104/aet.2024.6631.1814

water in South Africa due to large Mn ores deposits and intensive mining activities. Manganese occurs naturally and is the 12th most prevalent element in the earth's crust. However, anthropogenic activities, specifically mining, significantly contribute to the accumulation of Mn content in the environment. The most common oxidation states of Mn are Mn^{2+}, Mn^{3+}, Mn^{4+}, Mn^{6+}, and Mn^{7+}, with Mn^{2+} being the most stable state [3].

Manganese is essential for human health and plant metabolism. In humans, Mn is an essential dietary element, present as a coenzyme in several biological functions, including bone formation, boosting of the immune defense system, and a vital component of protein and enzyme [4]. As such, the deficiency of Mn in living beings results in many health issues, such as skeletal deformation and lack of collagen production, leading to delayed wound healing in animals and human beings; in plants, Mn is crucial in the photosynthesis process since it is responsible for the terminal photooxidation of water during the light reaction of photosynthesis [5]. Despite being very useful for human health and other living organisms, Mn is toxic at elevated concentrations, thus becoming a significant environmental and public health concern. Precisely, at elevated concentrations, Mn is toxic to humans, thereby resulting in many health effects. In adults, elevated concentrations of Mn cause a neurological disorder or manganism that resembles Parkinson's disease with symptoms such as tremors, gait problems, and facial muscle spasms [6]. In children, high concentrations of Mn are responsible for increasing intellectual impairment and reducing intelligence quotients. Since drinking water is the main pathway of Mn to human organisms, regulatory bodies, including the World Health Organisation (WHO) and South Africa Water Quality Guidelines (SAWQG), have set a maximum permissible concentration (MPC) of 0.02 mg/L of Mn in potable water [7]. In South Africa, Mn concentrations above the MPC set by the WHO and SAWQG were reported in the Mutangwi River by Madilonga et al. [8], surface and groundwater [9], Vhembe district by Edokpayi et al. [10], Spekboom River by Addo et al. [11], Dzindi River by Edokpayi et al. [7], Vaal River by Luus-Powell and Avenant-Oldewage [12]. In Russia, Matveeva et al. [3] reported very high concentrations of Mn in mining-influenced rivers and lakes.

Surface and groundwater are natural freshwater resources that are treated to remove PTEs and other pollutants prior to their distribution for domestic and industrial use [13]. In order to remove PTEs, including Mn in an aqueous solution, conventional techniques are commonly used, including filtration, precipitation, ion exchange, flocculation, coagulation, reverse osmosis, and adsorption [14, 15]. Amongst the above-cited water treatment technologies, adsorption is more advantageous since it is simple to design and, above all, economically sustainable. Adsorption is commonly applied to attenuate PTEs such as Mn in water and wastewater. In line with that, various adsorbents, including metals organic frameworks, modified biochar, and activated carbon, have been used for the removal of PTEs, including Mn, in water [16]. However, their escalation to the industrial level is difficult and complex due to their high cost and associated environmental and human health effects. As an alternative to current adsorbents, researchers and the scientific community in the water treatment field are constantly investigating the use of bio-sorbents. As such, agricultural by-products are being investigated due to their inexpensiveness and availability. Using agricultural by-products to remove PTEs in water will open the route for a circular economy approach (CEA) and environmental pollution control. Common agricultural by-products used as bio-sorbents to remove PTEs in contaminated water include banana peels (BPs), eggshells (ES), coconut shells (CCS), orange peels (OPs), sugarcane bagasse (SCB), and rice husks (RH) amongst others [17]. For instance, Molaudzi and Ambushe [18] investigated the efficacy of SCB and OPs in the attenuation of Pb(II) in contaminated aqueous solution; Mohan [19] assessed the potential of OPs and SCB for the elimination of Cu from industrial wastewater. In addition, Afolabi et al. [17] investigated the adsorption of Cu(II) and Pb(II) in binary systems using OPs.

As far as the authors of this manuscript are aware, OPs and SCB have never been investigated for the attenuation of Mn(II) in effluent samples. Exploring the use of OPs and SCB for the attenuation of Mn(II) in the effluent samples, as reported in this

manuscript, will appear as the first study of its kind. The adsorption efficiency of OPs and SCB was proven to be very high; they are cost-effective, always available, and easy to implement [20]. The use of agricultural waste, such as OPs and SCB, as low-cost bio-sorbents for water treatment, has dual benefits: (i) it valorizes agricultural waste, thus ensuring zero solid discharge (ZSD), and (ii) ensures environmental pollution control and opens the route for the concept of CEA. This study used state-of-the-art analytical techniques to characterize OPs and SCB; studies were also conducted to investigate the effect of pH, contact time, bio-sorbent dosage, and initial concentration of Mn(II) on bio-sorption.

2. Materials and methods

2.1. Acquisition of reagents

The analytical-grade reagents employed in this research were obtained from Merck, South Africa.

2.2. Acquisition and treatment of bio-sorbents

Orange fruits were purchased from a recognized vegetable shop (Food Lover's Market) in Johannesburg, and the sugarcane sticks were purchased from a sugarcane farm in Mpumalanga, South Africa, and taken to the University of Johannesburg, Auckland Park Kingsway (APK) campus. Once on campus, the orange fruits were peeled to obtain the OPs; the sugarcane sticks were peeled, and the fibular parts were pressed to extract the juice and obtain SCB. Both the OPs and SCB were washed with ultrapure deionized water from a MilliQ water purifier system with 18.2 MΩ/cm as resistivity. Then, they were air-dried in a controlled environment for two weeks, and ground using a Nima electric grinder (Osaka, Japan) to obtain a powder. The powder was sieved using a 5 µm pore size sieve, and particles of the same size obtained were used for the experiment.

2.3. Preparation of Mn(II) solutions

2.3.1. Preparation of 1000 mg/L Mn(II) solution

Manganese(II) sulfate monohydrate ($MnSO_4.H_2O$) was used to prepare a synthetic Mn(II) contaminated aqueous solution. A 1000 mg/L Mn(II) synthetic solution was created by dissolving 3.076 g of $MnSO_4.H_2O$ in 1000 mL volumetric flasks and topping it to its volume with ultrapure deionized water.

2.3.2. Collection of field water samples and characterization for initial Mn concentration

Acid mine water was supplied by a coal mine in Mpumalanga Province, South Africa. The AMD water was filtered before being analyzed by inductively coupled plasma optical emission spectroscopy (ICP-OES) to determine the initial Mn(II) content in AMD water. The filtered acid mine water was treated with pure SCB and OPs to explore the possibility of SCB and OPs binding Mn(II) ions with ions from other metal species present.

2.3.3. Preparation of calibration standard solutions for analysis using FAAS

Prior to the preparation of the standard solutions, a 10 mg/L solution was made by diluting 1 mL of the solution prepared in section 2.3.1 to 100 mL with ultrapure deionized water. The intermediate solution was used to prepare five standards of 0.1, 0.5, 1, 1.5, and 2 mg/L following the method described by Mestek [21], while ultrapure deionized water was used as a blank solution.

2.3.4. Adsorption experiment

To investigate the optimum adsorption conditions for OPs and SCB, the impact of pH, bio-sorbent dosage, and contact time on removing of 50 mg/L were assessed. The previously prepared bio-sorbent powder was added to the contaminated water. The solutions were filtered, with the content of Mn(II) quantified using FAAS. The content of Mn(II) adsorbed per unit of bio-sorbent powder mass at equilibrium (q_e) was calculated as illustrated in Eq.1 [22], while the RE of the bio-sorbent was calculated using Eq. 2 [23, 24].

$$q_e = \frac{(C_O - C_e)v}{W} \quad (1)$$

where Co is the content before adsorption (mg/L), Ce is the content after adsorption (mg/L),

V is the volume (L), and W is the mass used (g).

$$RE = \frac{C_i - C_f}{C_i} \quad (2)$$

where C_i and C_f are, respectively, the initial and final concentrations of Mn(II) in an aqueous solution.

2.3.5. Batch adsorption studies

The influence of pH, contact period, bio-sorbent amount, and initial metal ion concentration were investigated to determine the optimum conditions for the adsorption of Mn(II) using SCB and OPs. The sample preparation in this study was performed in 100 mL for both the simulated and AMD water solutions. The bio-sorbents were used individually and in homogenized combinations in batch studies. A Whatman filter paper with a 0.45 µm pore size was used to filter all the solutions.

2.3.6. Effects of pH variation on Mn(II) removal

The influence of pH was explored at different pH gradients (pH 3, 4, 5, 6, and 7). A pH beyond 7 was not explored due to the precipitation of Mn(II) at an alkaline pH range. The pH of each initial solution was 4.87, and the pH of each solution was adjusted accordingly to obtain the desired pH values. Into each solution, 0.03 g of bio-sorbent (OPs and SCB) was added, and the mixture was stirred at 500 rpm for 1 h with a magnetic stirrer. The solutions were then filtered, collected, and analyzed using FAAS, while the reacted bio-sorbent was characterized using different state-of-the-art characterization techniques.

2.3.7. Influence of contact time on removal of Mn(II)

The pH of the solution was adjusted to 5 to assess the contact time effect on Mn(II) removal, and 0.03 g of the bio-sorbent (OPs and SCB) was separately added into different beakers and stirred at 500 rpm for the designated contact period (10, 30, 60, 90, 120, 150, and 180 min). The ideal contact time for the removal of Mn(II) from water was obtained.

2.3.8. Influence of bio-sorbent dosage on removal of Mn(II)

The pH of the solution was adjusted to 5 to assess the influence of adsorbent dosage on Mn(II) removal, and 10 mL of 50 mg/L of the solution was transferred into a 100 mL beaker. A total of eight solutions corresponding to the eight different masses of adsorbent were used. The following dosage (0.01, 0.05, 0.1, 0.15, 0.2, 0.25, 0.3, and 0.35 g) of adsorbent (OPs and SCB) were added to each beaker, mixed for 1 h, and filtered. The filtrate was analyzed using FAAS to determine the Mn(II) concentration, while the residue was collected for reuse studies.

2.3.9. Investigation of the removal of 50 mg/L Mn(II) with a change in initial Mn(II) content

The impact of varying initial composition on the elimination of Mn(II) at different levels in a 100 mL solution was explored by creating synthetic water samples with initial Mn(II) content ranging from 10 to 200 mg/L. Every sample had a pH of 5, with the addition of 30 mg of SCB. The resulting mixture underwent 30 minutes of agitation before filtration and subsequent analysis using FAAS.

2.3.10. Removal of Mn(II) using combined SCB and OPs bio-sorbents

The study investigated the influence of blended SCB:OPs to evaluate and compare the efficiency of Mn(II) elimination when utilizing a combined mixture of SCB and OPs. This analysis also aimed to address scenarios in which one of these bio-sorbents might be limited due to seasonal fluctuations.

2.3.11. Influence of pH variation on Mn(II) removal

By modifying the acidity level from pH 3 to pH 7 with a dose of 50 mg SCB:50 mg OPs over a duration of 60 minutes, the influence of pH on the joint utilization of SCB and OPs for the extraction of 50 mg/L Mn(II) was examined. Following filtration and analysis through FAAS, the optimal pH for the extraction of 50 mg/L Mn(II) was identified.

2.3.12. The effect of contact time

The optimal pH was pH 7, and several contact periods were employed in removing 50 mg/L of Mn(II) in 100 mL using homogenized 0.1 g of SCB and OPs (1:1). The contact time range investigated for Mn(II) removal was between 10 to 180 min, and the ideal contact period was quantified after analyzing the solutions by FAAS.

2.3.13. Effect of bio-sorbent dosage on Mn(II) removal

Combining 0.1 g of homogenized OPs: SCB, the removal of 50 mg/L Mn(II) was examined. The homogenized OPs and SCB were divided in the bio-sorbent dosage ratio range of 9:1 to 1:9. After analyzing the solutions using FAAS, the ideal

dosage for the homogenized combination was determined.

2.3.14. Effect of initial metal ion concentration

Various aqueous solutions at different concentrations of Mn(II) were prepared to assess the influence of the initial Mn(II) concentration. The initial metal ion content was varied from 10 to 200 mg/L, with the pH of the solution maintained at 7. The two bio-sorbents were added to the solution at a 1:1 ratio. Subsequently, the mixture was stirred at 500 rpm for 180 min, followed by filtering and analysis for Mn(II) content using FAAS and the determination of RE at various concentrations.

2.3.15. Adsorption of Mn(II) in real water samples

To assess how the composition of the sample matrix influences the adsorption of Mn(II), the removal of Mn(II) in wastewater (acid mine water) using OP and SCB was investigated. The effectiveness of the bio-sorbent material in the presence of potential competing ions was examined by investigating the impact of a genuine water sample matrix. Before analyzing for Mn(II) concentration using ICP-OES, pure AMD water underwent filtration to establish the initial Mn concentration. Subsequently, 0.1 g of OPs, 0.1 g of SCB, and 0.1 g of the SCB:OPs combination (1:1) were applied to treat the AMD. The resulting solutions were filtered and subjected to FAAS analysis.

2.3.16. Characterization studies

Studies on characterization were conducted as a foundation for chemical species' fate post-adsorption; pure and water-reacted bio-sorbents Mn(II) were characterized using state-of-the-art characterization techniques. Precisely, the functional groups on SCB and OPs were conducted using Fourier transform infrared spectroscopy (Bruker Tensor 27, Shimadzu, Kyoto, Japan). The SDT Q600 V20.9 Build 20 instrument (New Castle, USA) was employed for both SCB and OPs to examine the thermal stability. Morphology and elemental composition were carried out using scanning electron microscopy energy-dispersive X-ray spectroscopy (Brno-Kohoutovice, Czech Republic). Enhancing sample conductivity was achieved through carbon coating using a coater (Q300T ES, Quorum, Japan). Lastly, the crystalline nature of SCB and OPs was disclosed using an X-ray diffractometer (XPERT-PRO, PANanalytical, Netherlands), and surface charges were analyzed using a zeta potential analyzer (ZEN3600, MALVERN Nano-ZS, Randburg, South Africa).

2.3.17. Regeneration studies of bio-sorbents (OPs and SCB)

Regeneration is crucial for an adsorbent to be applied in large-scale applications. When evaluating the viability of a sorbent, it is important to consider two main characteristics: the ability of innovative sorbents to regenerate under convenient conditions and their degree of reusability [25]. Therefore, this study attempted to reuse these bio-sorbents to enhance their relevance in industrial applications. Consecutive adsorption/desorption cycles in aqueous acidic solutions were used to test the bio-sorbent's reusability. The desorption experiments at the same amount of loaded bio-sorbents were carried out using 30 mL of 0.3 M HNO_3 solutions for an hour to regenerate the ion sorption capacity; the sorption studies were carried out in 100 mL of 50 mg/L Mn(II) for 0.1 g of bio-sorbent. The composite bio-sorbent was washed countless times with deionized water to reach the neutral pH and then reused for a new cycle of sorption. The adsorbent doses of 0.1 g for SCB, OPS, and homogenized SCB and OPS (1:1) were used.

2.3.18. Limit of detection, limit of quantification and linearity

The lowest amount of an analyte that may be consistently detected and separated from background noise is measured by the limit of detection (LOD). The LOD was determined through the examination of 10 reagent blanks. The LOD represents the concentration at which the signal surpasses the background signal thrice. Consequently, the LOD was computed by multiplying the standard deviation of the mean by 3 (3σ), while the LOQ was calculated by multiplying the standard deviation of the mean of the 10 reagent blanks by 10 (10σ) [26]. The linearity determines the concentration of an analyte that can be determined from the linear calibration curve. The calibration plot serves as a regression model utilized for estimating the concentrations of

an analyte whose values are unknown, relying on the instrument's response to calibration standards [26]. The coefficient of determination (R^2) value from the analysis of calibration standards allows for extrapolation, and the unknown concentrations of analytes can be determined.

2.3.19. Determination of method of accuracy and precision

The accuracy of a method determines how close the response values are to the reference values, and the precision of a method is a measure of how close the instrumental responses are to each other. The percentage relative standard deviation (%RSD) of the analysis of triplicates was used to evaluate the method's precision. This means that a lower %RSD is a clear indication of the method's precision, as it indicates that the triplicate analysis done by the instrument gives responses that are very close to each other [27]. As a result, the repeatability of the method is also high. Standard reference materials are often used for method validation and determining the method's accuracy. Without certified reference materials, spiking is used as suggested by the United States Environmental Protection Agency method [28]. Therefore, the accuracy was determined by spiking the simulated and real solutions with a known concentration of Mn and determining the percentage recovery after analysis with FAAS. The accuracy of the method was evaluated at 1×LOD and 10×LOQ.

2.3.20. Quality assurance and quality control (QA/QC)

In this research, the QA/QC procedure was applied to warrant the generation of trustworthy results. This QA/QC protocol encompassed the handling and conservation of samples, the experimental procedures, and the analytical processes. Every experiment was carried out in triplicate, and if the difference was less than 5%, the mean values reported were considered satisfactory.

3. Results and discussion

3.1. Effect of pH on Mn(II) removal

The effects of pH on Mn(II) removal were investigated for individual and combined bio-sorbents, and the results are shown in Figure 1.

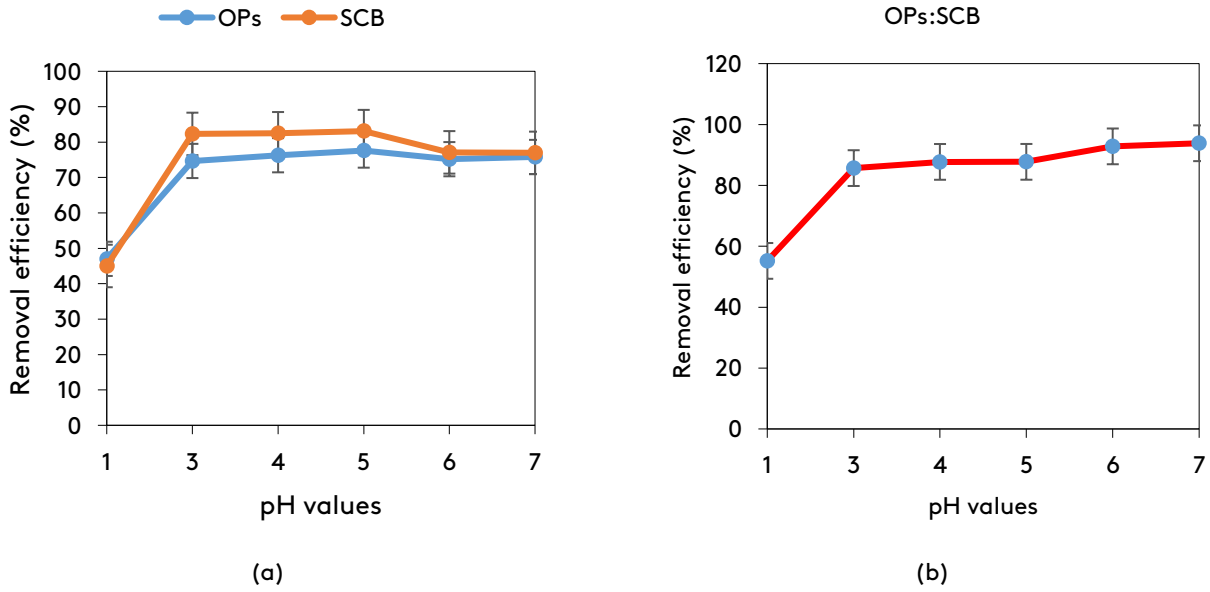

Fig. 1. Effect of pH variation on adsorption capacity: a) individual and b) combined bio-sorbents.

The findings from Figure 1 revealed that the RE increased with the rise in pH for both individual and combined bio-sorbents. For individual bio-sorbents, the RE at pH 1 was 45.01% and 47.02% for SCB and OPs, respectively, while the RE at pH 1 was 55.2% for the combined bio-sorbents. For the individual bio-sorbents, as the pH was adjusted to 5, the RE significantly increased to 77.61 % and 83.1 % for SCB and OPs, respectively, and further dropped when the pH was adjusted to 6 (pH 6). Thus, pH 5 was the optimum pH level at which each bio-sorbent could be effective in Mn(II) removal

(Figure 1a), while the RE became constant at pH 6 with the combined bio-sorbent (Figure 1b). In fact, the pH had a huge effect on the RE of the bio-sorbent since the rise of pH led to increasing oxidation of the bio-sorbent materials, which became negative as the pH increased. The minor RE at a low pH level might result from competition between the H^+ produced by protonation of the bio-sorbents active sites and the Mn(II) ions. When the combination of OPs:SCB was used, the maximum adsorption pH was pH 6, which was consistent with the fact that there were fewer H^+ ions at this pH value. Within the macropores and micropores of the internal structure of the bio-sorbents, PTEs were more easily diffused and entrapped due to the large porosity and surface area of the SCB and Ops, which enhanced the continuous attenuation of hydrolysed Mn(II) anions across the pH gradients as revealed by Mohan [19] who used OPs and SCB for the attenuation of Ni from contaminated aqueous solution.

Furthermore, once the pH was above the PZC (2.1 for OPs and 2.2 for SCB), bio-sorbents bore a negative charge, thus facilitating their attraction to positively charged Mn(II). As a result, Mn(II) was easily trapped in the pores [29]. The low RE at pH ≤ 4.5 could be credited to the effects of competitiveness between excess H^+ ions and Mn(II) in the solution [30]. According to Ali [31], the ionization degree of the functional groups and the speciation of metal ions also facilitate the attenuation of metal ions using bio-sorbents. The attraction of Mn(II) to the surfaces of both SCB and OPs might also be attributed to the electrostatic attraction because of positively charged Mn(II) at any pH lower than 7.5 [32]. According to the zeta potential analysis results, as the pH increased above the pH_{pzc}, which occurred at 2.2 for SCB and at 2.1 for OPs, the bio-sorbents exhibited a negative charge, and their attraction for positively charged Mn(II) increased; thus, confirming the surge in RE with a rise in pH values.

3.2. Influence of contact time on Mn(II) removal

The influence of the contact period on Mn(II) removal was investigated for individual and combined bio-sorbents, and the findings are shown in Figure 2.

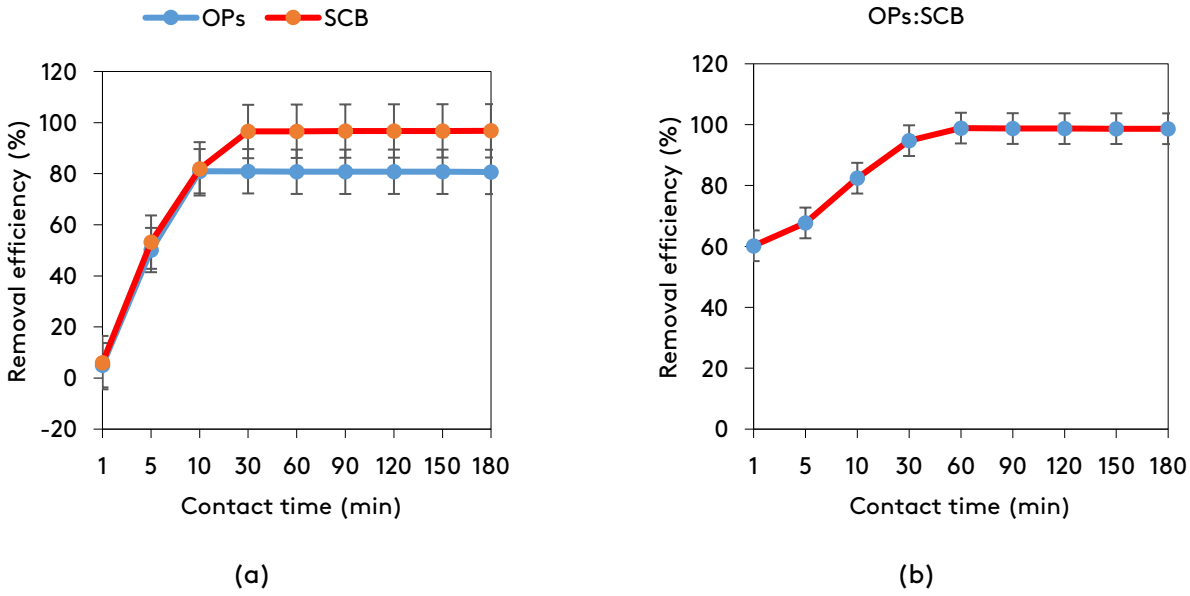

Fig. 2. The influence of contact time on the removal of Mn(II): a) individual and b) combined bio-sorbent.

Figure 2 depicts that the increases in contact period also led to the increase of RE for both individual and combined OPs:SCB. However, the optimum contact time differed for the bio-sorbent, with OPs reaching the optimum contact time at 10 min with a RE of 96.5% RE, whereas the optimum contact period for SCB was 30 min, with an optimum RE of 81.89%. The ideal contact time was 60 min with an RE of 98.88% for the combined OPs:SCB. The significant increase in RE before the optimum contact period could be credited to active sites available on the bio-sorbent surface. The prolonged

contact time led to the complete occupation of active sites and the slowing down of the adsorption capacity of the bio-sorbent [33]. Higher removal levels were observed at 60 min following 50 mg/L of Mn(II) sorption onto 0.1 g of SCB and OPS in a 1:1 ratio combination. Figure 2 shows a significant increase in RE at the beginning of the experiment. The ideal contact time was 10 min and 30 min for OPs and SCB, respectively, for the individual bio-sorbent and 60 min for the combined bio-sorbent. The high RE from the beginning of the experiment was the result of the bio-sorbent's high surface area and reactive surface site towards the Mn(II) ions. As the contact period increased, available active sites were reduced, leading to slow adsorption capabilities; an equilibrium point was attained at 30 min for individual bio-sorbents (Figure 2a) and at 90 min for combined bio-sorbent (OPs:SCB) (Figure 2b). The adsorption rate will eventually stabilize or slow down due to the solute's slower diffusion into the interior of the bio-sorbent, as reported by Mayerhofer et al. [34]. After the optimum contact time, the RE of both individual and combined bio-sorbents remained relatively constant or slightly decreased despite the prolonged contact time of 180 min. The stability in the RE of bio-sorbent after the optimum contact time might also be attributed to the saturation of active positions, after which the prolonged contact time did not have any effect on the adsorption capacity of bio-sorbent, thereby corroborating with the finding reported by Rudi et al. [27]. They found that due to the available sites, the RE of bio-sorbent (OPs and SCB) had two-phase phenomena involving a significant increase of RE before the optimum contact time and stability or decrease after the optimum contact time.

3.3. Influence of bio-sorbent dosage on the removal of Mn(II)

The solution pH was adjusted to 5, and the effects of bio-sorbent dosage were investigated by varying the dosage of OPs and SCB in the following order: 10, 30, 50, 100, 170, and 200 mg. The effect of initial Mn(II) content was assessed at a concentration that varied between 10 – 100 mg/L, and the results are illustrated in Figure 3.

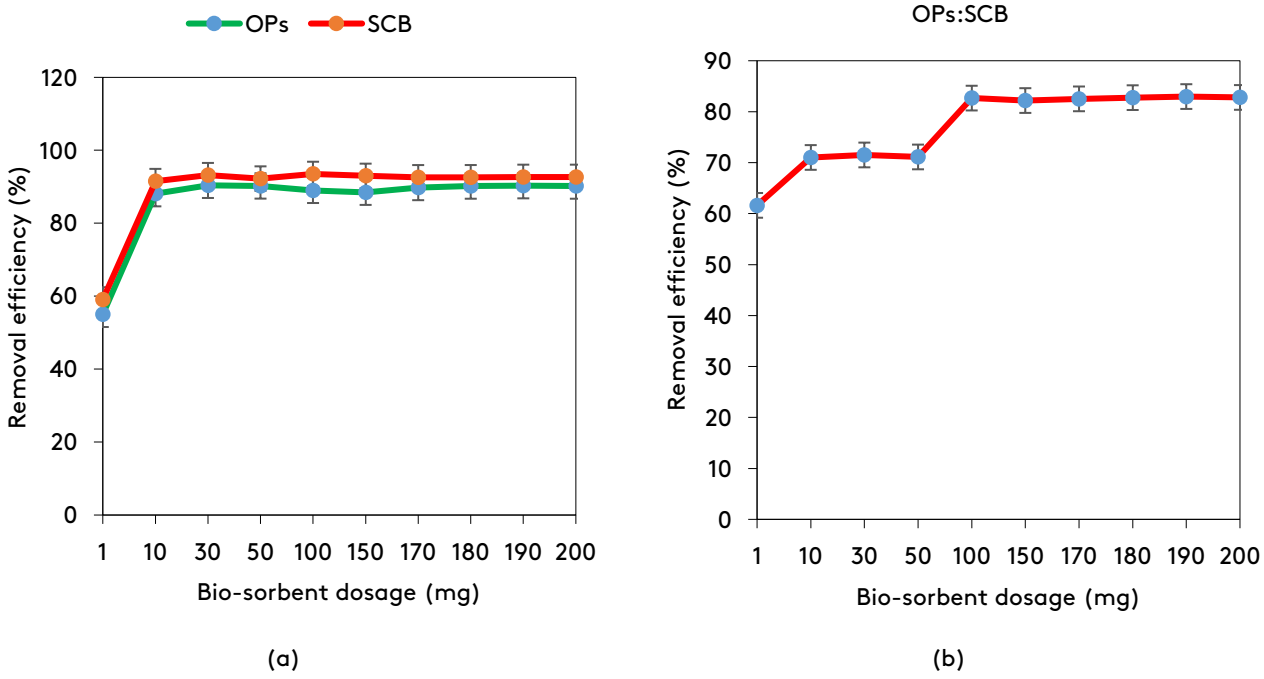

Fig. 3. Effects of bio-sorbent dosage on the adsorption capacity.

As seen in Figure 3 (a, b), an increase in the bio-sorbent dosage led to a significant increase in RE. This could be credited to elevated concentrations of active sites resulting from the higher dosage of bio-sorbent [35, 36]. The increase of active sites resulted in a consistent number of oxygen-bearing functional groups, including alcohol ($C_nH_{2n+1}OH$), carboxylic acid ($C_nH_{2n+1}COOH$), and esters (RCOOR'), as revealed by the FTIR analysis. The OPs and SCB followed the same trends despite the difference in RE in bio-sorbent dosages. In addition, the results revealed that 30 mg of both OPs and SCB significantly increased the RE to 93.41% and 93.18%, respectively. The further increase in bio-sorbent dosage to 200 mg allowed a slight increase in the RE to 94.34% and 93.95% for OPs and SCB, respectively. The findings indicate that OPs showed a higher RE than SCB with the same quantity of bio-sorbent. The results further revealed that combined bio-sorbent at a 1:1 ratio in every contact time also led to a significant RE increase, with the optimum dosage of 100 mg corresponding to a RE of 82.67% (Figure 3b). This was a definite indication that combining OPs and SCB had little influence on the sorption of Mn(II), which might be explained by the fact that both SCB and OPs have similar physicochemical qualities, as revealed by characterization results (FTIR and TGA), and confirming findings reported by Bade et al. [37].

3.4. Effect of initial metal concentration on the removal of Mn(II)

The influence of the initial metal ion concentration on the attenuation of Mn(II) was investigated over a series of concentrations ranging from 1 to 200 mg/L, as shown in Figure 4.

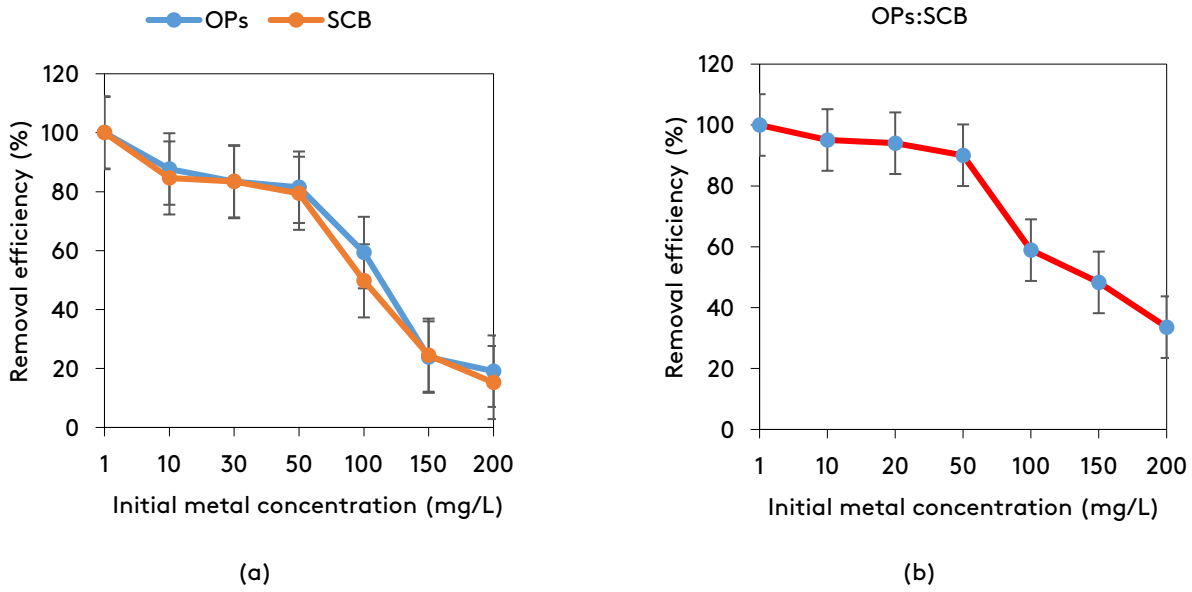

Fig. 4. Effect of metal ion concentration on the removal of Mn(II): a) individual and b) combined bio-sorbents.

The outcomes revealed that with an initial Mn(II) content of 1 mg/L, there was 100% RE for both individual and combined bio-sorbents and could be the result of abundant active sites in the surface of bio-sorbents compared to low metal ion concentration leading to an increasing affinity for metal ions. Inversely, as the content of Mn(II) increased, the RE decreased. This occurred because metal ion concentrations easily impact metal ion diffusion through to the surface of bio-sorbents. The diffusion of metal ions from the solution to the surfaces of the bio-sorbents was, therefore, accelerated by an increase in the metal ion concentrations [38, 39]. All bio-sorbents were limited in the number of active sites they could saturate at a given concentration, and this could explain why the RE of Mn(II) ions decreased at higher concentrations. The results further revealed that after 200 mg/L, the RE of both the individual

and combined bio-sorbents became relatively constant.

3.5. Adsorption of Mn(II) in real water samples

The adsorption of Mn(II) from feed AMD was evaluated using individual and combined bio-sorbents (SCB and OPs), as shown in Figure 5.

The results from Figure 5 show that the adsorption of Mn(II) from acid water by OPs was 37.01%, while SCB gave a percentage removal of 37.78%. The combined SCB:OPs resulted in the highest removal of 42.44%. This indicated that the adsorption of Mn(II) by the bio-sorption of SCB and OPs decreased in the presence of competitor ions since the competition was created by other metal ions for the active sites on the surface of the bio-sorbents. The acid mine water was mine wastewater very rich in metals (Al, Cu, Fe, Mn, Ni, Pb, Mg, and Zn) and sulfate ions (SO_4^{2-}) [23], [24], [40], and [41]. As a result, when the AMD water was treated with SCB and OPs, a significant quantity of these metals were adsorbed due to the competition of mobile ions to occupy active sites, leading to low RE, as reported in this study.

3.7. Characterisation studies results

3.7.1. Zeta potentials results of pure OPS and pure SCB

Zeta potential analyses were done for the pure bio-sorbents, and the results are presented in Figure 6.

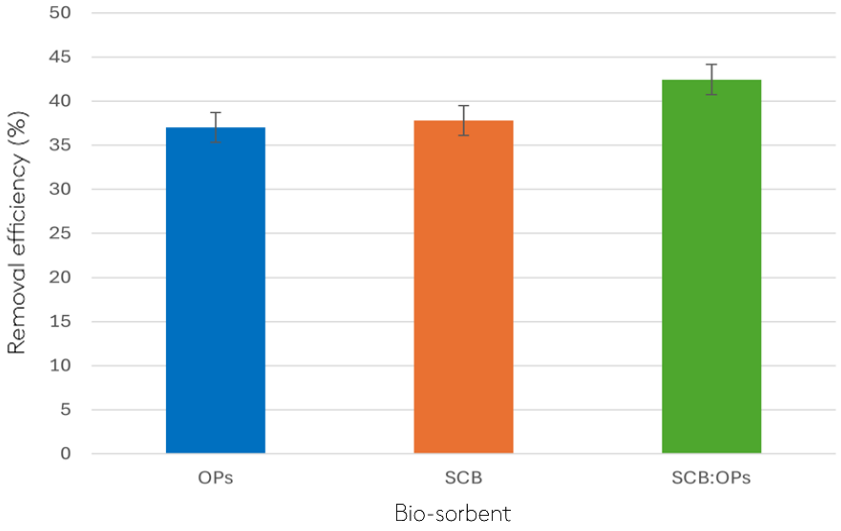

Fig. 5. Effect of sample matrix on Mn(II) removal by individual and combined SCB:OPs.

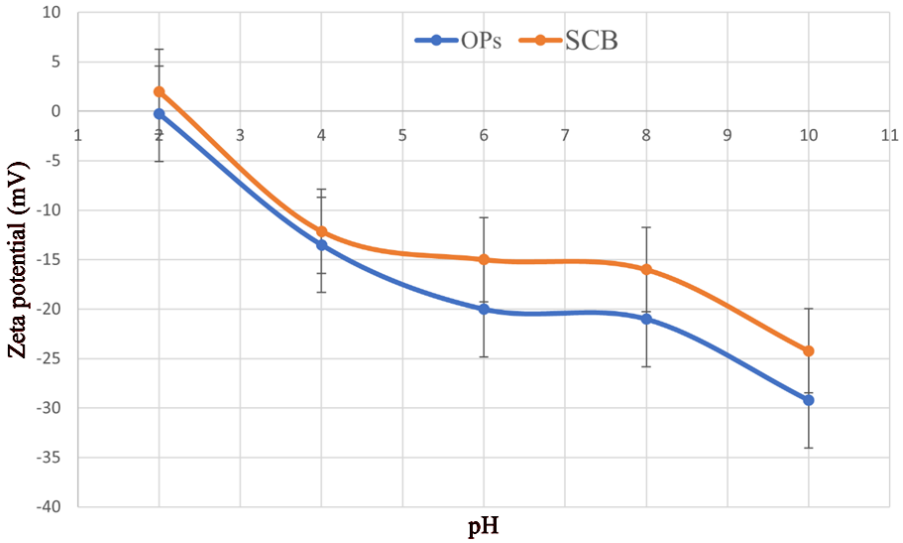

Fig. 6. Zeta potential of orange peels and sugarcane bagasse.

Zeta potential was used to determine the charge of the adsorbent at different pH levels. The point of zero charge (PZC) is the pH level corresponding to the point where the adsorbent has zero as a net surface charge [42]. The PZC of the OPs was found at 2.1, while the PZC of SCB was found at 2.2, meaning all charges above the PZC were negatives. The PZC is influenced by surface protonation and deprotonation, which alters the surface charge of the adsorbent. Protonation and deprotonation are influenced by hydrogen ions (H^+) and hydroxide ions (OH^-), which change the surface charge of the adsorbent in the aquatic environment. Hydroxide ion increases the negativity level of the adsorbent, thus creating a negatively charged double layer, while the H^+ ions create an acidic solution, thus increasing the positivity of the double layer [33]. As illustrated in Figure 6, the zeta potentials of OPs showed negative values across the studied pH range, indicating that the surface of OPs was well-suited for interacting with cations. The ability to bind Mn(II) was significantly improved due to the pH increase and the continuous negative zeta potential values. The zeta potential of sorbent materials highly influences the sorption of ions. As such, cations are attracted by the sorbent materials bearing a negative charge, while anions are attracted by sorbent materials bearing a positive charge [43].

3.7.2. Thermogravimetric analysis

The TGA was performed to study the mass loss events of OPs, SCB, and combined OPs:SCB following the temperature increase from 0 to 1000 °C, and the outcomes are shown in Figure 7.

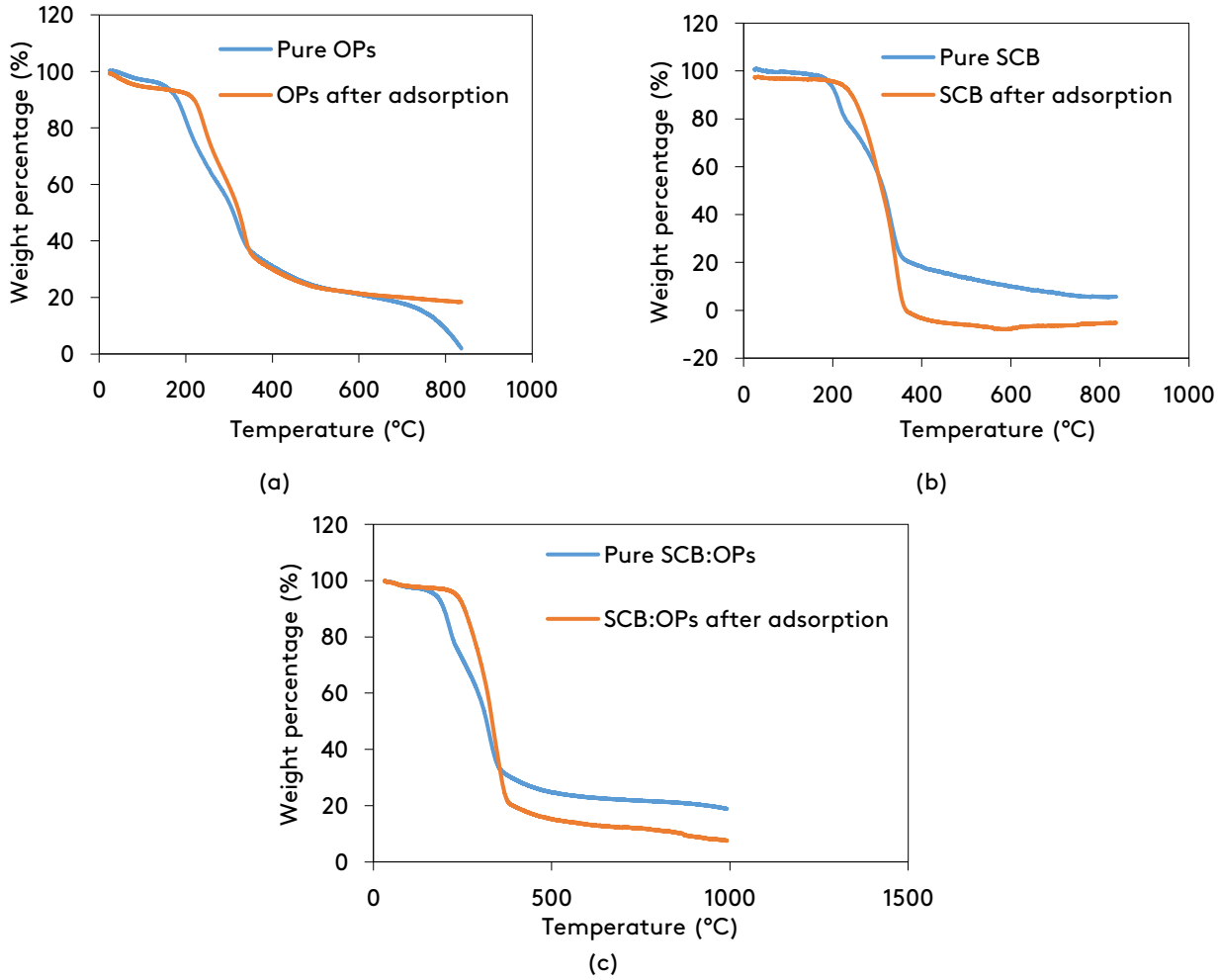

Fig. 7. Thermogravimetric results of a) pure and water-reacted orange peels, b) pure and water-reacted sugar cane bagasse, and c) pure and water-reacted combined OPs:SCB.

The TGA results of the pure and reacted OPs displayed different patterns. The TGA results of pure OPs presented two mass-loss events: the first mass-loss event occurred between 35 °C and 260 °C where approximately 10.24% of OPs was lost, while the second mass-loss event occurred between 260 °C and 770 °C, corresponding to approximately 77.94% of mass lost. In the first mass-loss event, the loss of humidity and volatile matter was observed, whereas the decomposition of biomass occurred between 260 and 770 °C, leading to the degradation of lignin and hemicellulose. This merely means OPs mostly consisted of cellulose, followed by lignin and hemicellulose in terms of chemical makeup. However, after Mn(II) adsorption, the TGA of OPs showed three mass-loss events, which could be explained by the presence of Mn(II) adsorbed by OPs. In fact, Mn doping or impurities introduced in the aqueous solution were adsorbed by OPs, thus requiring high temperatures for their degradation. The third mass-loss event occurred above 770 °C and might be credited to the degradation of Mn(II) and its associated impurities, corresponding to 4.06% of mass lost. According to Morais et al. [29], the mass ratio of the primary components of the bio-sorbents, such as hemicellulose, cellulose, and lignin, determines how quickly they degrade under heat conditions, as illustrated in Figure 7a. The finding also revealed that 20% of the material was still intact after coming into contact with water. Given that metals are difficult to decay, this might be a sign of the presence of Mn(II). The weight loss patterns were very similar between 0 ˚C to 650 ˚C, which still confirmed the mass loss of the different components of OPs. However, a constant weight was observed after 800 ˚C. This could be an indication of the presence of Mn because metals are hard to degrade since only metallic and metal oxides exist after 800 ˚C, which confirmed the presence of Mn in the OPs after contact with water [43].

Figure 7b depicts one mass-loss event for both the pure and water-reacted SCB; however, at different temperatures. The mass-loss event occurred between 153 and 780 °C for pure SCB and between 200 and 930 °C for water-reacted SCB. This merely means humidity and biomass were lost in a single mass-loss event for both pure and water-reacted SCB. Biomass and its structural components (hemicellulose, pectin, lignin, and cellulose), which are degraded at different temperatures, were lost throughout the mass-loss event between 200 and 350 °C for hemicellulose and between 250 and 500 °C for cellulose, while lignin was degraded between 370 and 950 °C [44]. The results further revealed that water-reacted SCB required higher temperatures than pure SCB to degrade humidity and biomass, and this might be attributed to the presence of Mn(II) and its impurities adsorbed by SCB. Contrary to OPs, the TGA results of the pure and reacted SCB displayed the same patterns, and this might be credited to the SCB structure, which favoured the cohesion between the cell walls, thereby rendering the degradation more complex [44].

The TGA analysis results of the combined SCB:OPs following the increase of temperature from 0 to 1000 ˚C are shown in Figure 7c. The results demonstrated that the thermal degradation of the different components of the combined SCB:OPs before and after adsorption showed similar weight loss events. They were also identical to the TGA of the individual bio-sorbents. The first region of the TGA curve ranged from 30 to 200 ˚C for both graphs. The elimination of bound and free moisture, as well as the minor evaporation of volatile matter, were responsible for this [38]. The greatest devolatilization occurred in the second region between 200 and 850 ˚C. As stated, the degradation of cellulose and hemicellulose occurred between 200 ˚C and 350 ˚C. The subsequent mass loss in this part represented the breakdown of cellulose followed by the degradation of lignin and pentosane [44]. After adsorption, the TGA showed a slow degradation of the components in SCB:OPs because their pores were filled with metal ions, which were extremely hard to degrade, resulting in slower thermal degradation [35].

3.7.3. Fourier transform infrared spectra

The FTIR analysis of pure and reacted bio-sorbents was conducted for OPs, SCB, and combined SCB:OPs, and the results are shown in Figure 8.

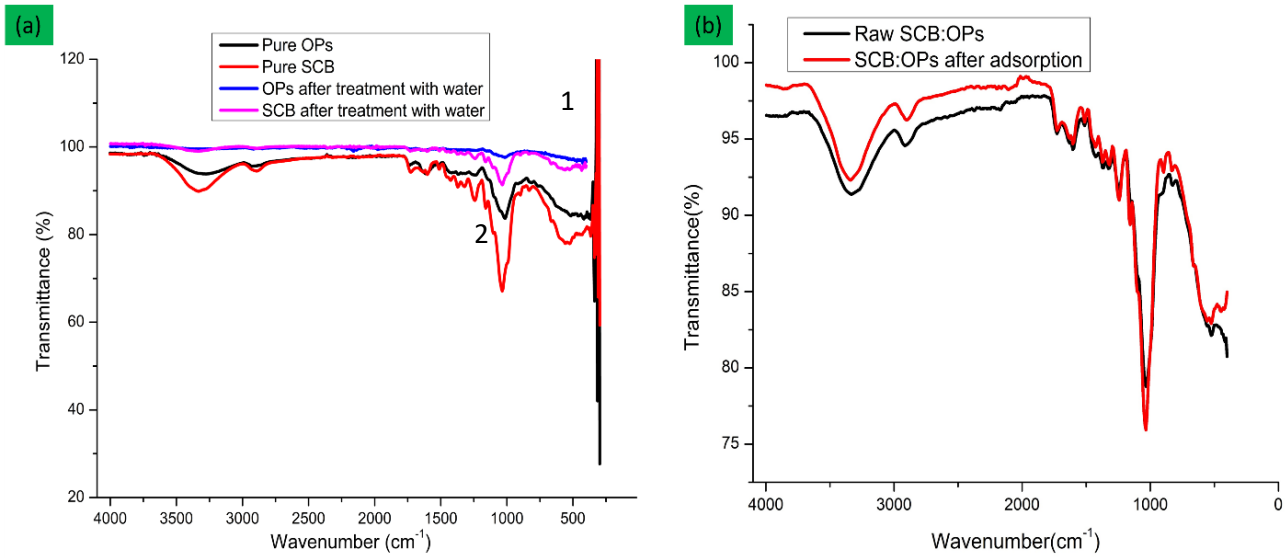

Fig. 8. FTIR results of a) pure and water-reacted orange peels and sugarcane bagasse and (b) combined orange peel sugarcane bagasse.

The FTIR analysis of SCB was performed, and the results of pure and water-reacted SCB are shown in Figure 8a$_1$. When comparing the two spectra, there was vibration for the pure and water-reacted SCB at 500 cm^{-1} and 1000 cm^{-1}. The bending vibration at 500 cm^{-1} corresponded to metal halogen (M-X), which corresponded to lignin, cellulose, and hemicellulose or polyose. The peak at 1000 cm^{-1} represents the Si-O functional group, thus indicating the presence of silica in both pure and water reacted SCB. Both spectra showed a series of vibrations with a series of peaks at 1100 cm^{-1}, 1225 cm^{-1}, 1300 cm^{-1}, and 1500 cm^{-1} corresponding to the unsaturated ether group C=O=C, which is a glycosidic ether band vibration. The vibration with peaks at 1600 cm^{-1} and 1810 cm^{-1} indicated the unsaturated alkene functional group C=C, thus confirming the presence of cellulosic β glycosidic linkages [44]. The FTIR spectrum of water-reacted SCB revealed the peaks at 1800 cm^{-1} and 4000 cm^{-1}, with a weak vibration peak at 3500 cm^{-1} corresponding to the adsorption of Mn(II) by SCB, thereby corroborating with findings from previous studies [45]. In pure SCB, the results revealed a doublet with peaks at 2780 cm^{-1} and 3295 cm^{-1}, corresponding to the presence of O-H groups.

The FTIR spectra of pure OPs and Mn(II) reacted OPs showed significant differences. As seen in Figure 8a$_2$, the broad peak at 3375 cm^{-1} indicated the presence of the O-H functional group, which is an intermolecular hydroxyl group made of alcohols and phenols from hemicellulose and pectic acid, thus confirming the results reported by Afolabi et al.[17] when they investigated the efficacy of OPs for the attenuation of Cu and Pb in a binary system. The peaks at 2800 cm^{-1} in pure OPs and at 2350 cm^{-1} after adsorption were significant for the presence of the C-H functional group in cellulose in the OPs. The vibration observed at 1780.00 cm^{-1}, 1600.98 cm^{-1}, and 1509.45 cm^{-1} in pure OPs consisted of the unsaturated carboxylic group C=O stretching from the carboxylate groups and carboxylic acid. The broad peak at 1000 cm^{-1} corresponded to C-O stretching vibration, confirming the presence of cellulose and hemicellulose in OP material.

Figure 8b presents the FTIR results of the combined OPs:SCB, and it follows that there are alterations or changes related to the interaction of Mn(II) in solution with the functional groups found on the surface of the bio-sorbent [22]. The adsorption monograms showed a significant shift that was unique to the adsorption of Mn(II) and contained peaks (2800 cm^{-1} and 3300 cm^{-1}) that indicated the O-H and C-O-H stretching; this FTIR spectrum is like the FTIR spectra of the pure SCB and OPs individually. This demonstrated that hydroxyl and carboxyl groups were crucial in the Mn(II) adsorption. The combined bio-sorbents' surface hydroxyl and carboxyl groups indicated that these bio-sorbents could adsorb positively charged metal ions [46].

3.7.4. SEM-EDS results of bio-sorbents

3.7.4.1. SEM-EDS results of pure and reacted bio-sorbents (OPs and SCB)

To understand the interaction of bio-sorbent with Mn(II), SEM-EDS analysis of the pure and reacted bio-sorbent was performed, and the results are shown in Figure 9.

Figure 9 (a, b) shows a noticeable difference in morphology between the pure OPs (Figure 9a) and water-reacted OPs (Figure 9b), as reported by Buthiyappan et al. [43]. The morphological properties of the pure OPs showed a foliage-like and shaped structure. However, after contact with water, the SEM image showed irregular and porous mass occupying the entire surface, and this might be attributed to the presence of Mn, as confirmed by EDS results. The EDS results showed the difference in the mineral phase in elemental composition. The elements C, O, K, and Ca were present in the pure OPs in amounts of 59.9%, 42.3%, 1.1%, and 0.7%, respectively, thereby demonstrating that the OPs were pure. However, after contact with water, C, O, P, Ca, and Mn were present in the OPs in the following percentages: 57.2%, 42.1%, 0.5 4%, 0.3%, and 3.49%, respectively, which confirmed the adsorption of Mn(II) by the OPs. On the other hand, the SEM images of the pure and water-reacted SCB (Figure 9 c, d) showed a perceptible dissimilarity in morphology. The SEM image of pure SCB showed less thickening mass compared to water-reacted SCB, which showed a sort of palette on the whole surface. These SEM images clearly demonstrate that the contact of SCB with water and specifically with Mn(II) had affected the morphological structure as well as the chemical composition, as evidenced by the difference in mineral phase from the EDS results. In pure SCB, C, O, Si, and K were present in the following percentages: 57.25%, 42.1%, 0.5%, and 0.3%, respectively. In the water reacted SCB, C, O, Si, and Mn were present at 54.83%, 44.21%, 0.61 % and 0.35%, respectively, confirming that OPs and SCB adsorbed Mn(II). The SEM-EDS results also showed that OPs were better bio-adsorbers compared to SCB; a higher percentage of Mn on the surface of OPs after adsorption confirmed this. Similar results were obtained by Dey et al. [44] when they used OPs as bio-sorbents for ammonia and nitrates in wastewater.

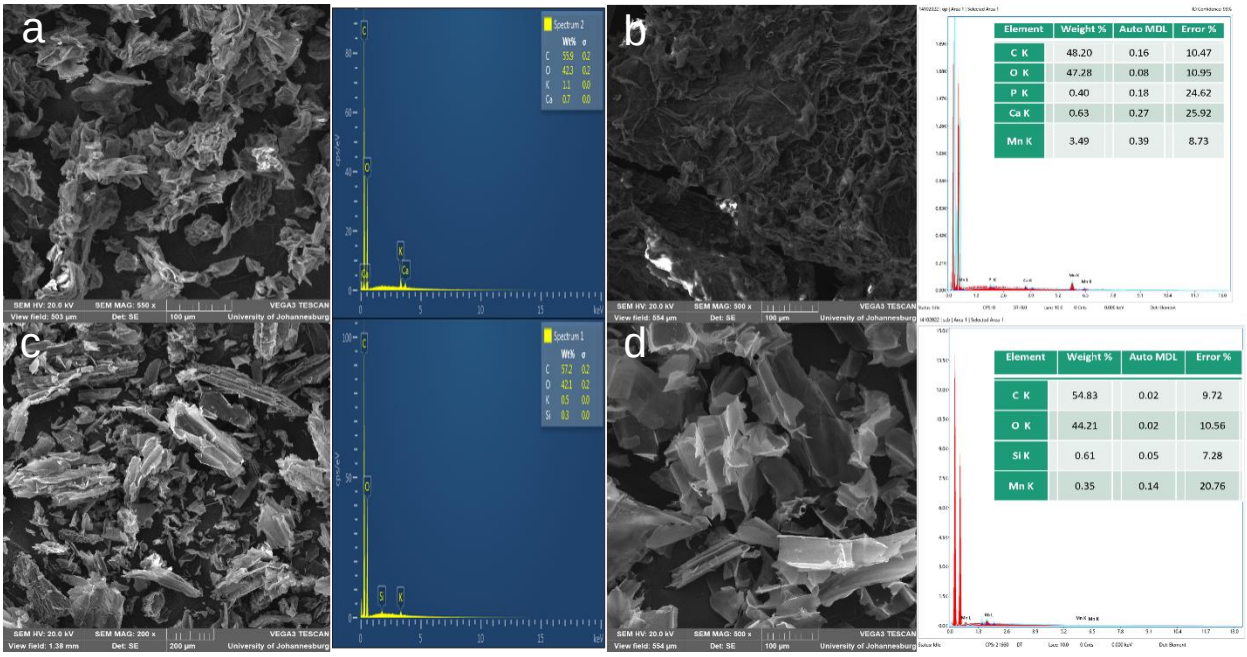

Fig. 9. SEM-EDS results: a) pure OPs, b) water-reacted OPs, c) pure SCB, and d) water-reacted SCB.

3.7.4.2. Scanning electron microcopy-energy dispersive X-ray spectroscopy results of combined pure and reacted SCB:OPs

The structural morphology and chemical compositions for the combined pure SCB:OPs and

combined reacted (OPs:SCB) are shown in Figure 10.

These SEM images unveil the OP pores and morphology, which were altered due to the presence of Mn(II) ions (Figure 10a). This is credited to the formation of new surface features following the combination of the bio-sorbents, which enhanced the adsorption of Mn(II) onto the surface of the combined SCB:OPs. Using a combination of these bio-sorbents increased the adsorption of bio-sorbents, as evidenced by the notable increase of Mn percentage (13.1%) in the EDS analysis following adsorption. This percentage stands in contrast to the individual percentage values of Mn, as shown in Figure 9, with 3.49% Mn using OPs and 0.35% Mn using SCB. For example, the EDS results showed that OPs had a higher oxygen content compared to SCB, while SCB boasted a superior surface area, according to a study by Lemessa et al. [35]. Therefore, combining these bio-sorbents resulted in a biomass with a combination of these properties. As a result, more adsorption was observed. This was reinforced by the optimization outcomes, which demonstrated increased RE when employing the combined SCB:OPs, as indicated in section 3.5. Under identical experimental conditions, the SCB:OPs combination exhibited a greater Mn(II) removal percentage. These results align with the findings of research conducted by Molaudzi and Ambushe [18], thus confirming that the combination of SCB and OPs enhanced the RE.

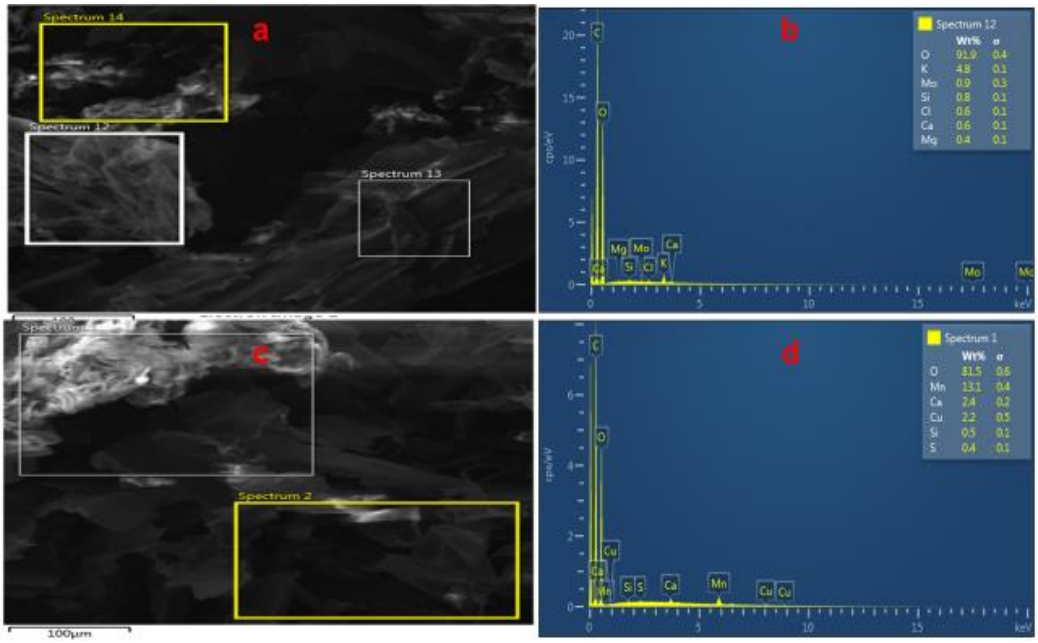

Fig. 10. SEM-EDS results: a-b) pure combined OPs:SCB and c-d) water-reacted combined OPs:SCB.

3.7.5. Powder X-ray diffraction results

3.7.5.1. Powder X-ray diffraction results of pure and reacted OPs and SCB

The p-XRD analysis was performed to determine the crystallinity of the materials of pure and water reacted bio-sorbents, and the results are shown in Figure 11.

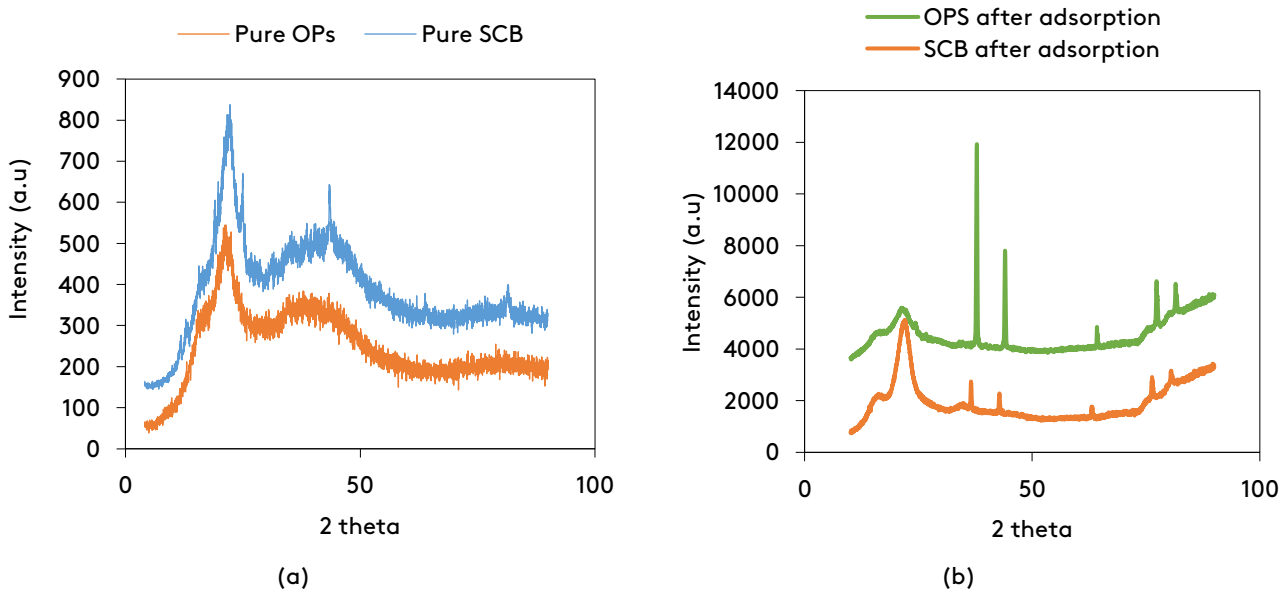

Fig. 11. Powder X-ray diffraction results: a) pure and water reacted OPs and b) pure and water reacted SCB.

The p-XRD of pure OPs and SCB diffractograms displayed a similar pattern, however, with a series of peaks found at 2θ = 15° and 2θ = 25° for SCB, which may indicate vitreous material such as solid, non-crystalline unstable matter [38]. In addition, the peaks at 2θ = 45° and 2θ = 82° were an indication of the quartz, as revealed by the previous studies. For pure OPs, the pattern revealed a peak at 2θ = 16°, which may indicate hemicellulose, while the peak at 2θ = 20° might indicate cellulose or quartz, as confirmed by the SEM-EDS results. Similar results were obtained in previous studies with the characterization of pure OPs [18]. After the reaction with water, the pXRD of OPs and SCB showed various peaks. The peaks at 2θ = 22.5° indicate non-crystalline plant material for both OPs and SCB. After 2θ = 35°, however, various peaks appeared for both the OPs and SCB at different intensities. For OPs, there was a series of peaks at 2θ = 38, 44, 2θ, 65 78, and 82°, while the series of peaks for SCB appeared at 2θ = 37.5, 43, 63.5, 77, and 81°. As revealed by the SEM-EDS results, the series of peaks for both OPs and SCB might indicate the presence of Mn(II) in bio-sorbent materials. Furthermore, the difference in intensity was confirmed by the quantity of Mn(II) in the bio-sorbent (3.49% for OPs and 0.35% for SCB).

3.8. Regeneration of SCB and OPs

This study attempted to reuse these bio-sorbents to enhance their relevance in industrial applications. Consecutive sorption/desorption cycles in aqueous acidic solutions were used to test the bio-sorbent's reusability. The desorption experiments at the same amount of loaded bio-sorbents were carried out using 30 mL of 0.3 M HNO_3 solutions for an hour to regenerate the ion sorption capacity; the sorption studies were carried out in 100 mL of 50 mg/L Mn(II) for 0.1 g of bio-sorbent. The obtained composites were cleaned repeatedly with de-ionized water to reach the neutral pH and then reused for a new cycle of sorption. The bio-sorbent doses of 0.1 g for SCB, OPS, and homogenized SCB and OPS (1:1) were used. The solutions were stirred to the ideal contact time and ideal pH and filtered before being analysed by FAAS. The results for the regenerations of OPS and SCB are shown in Figure 12.

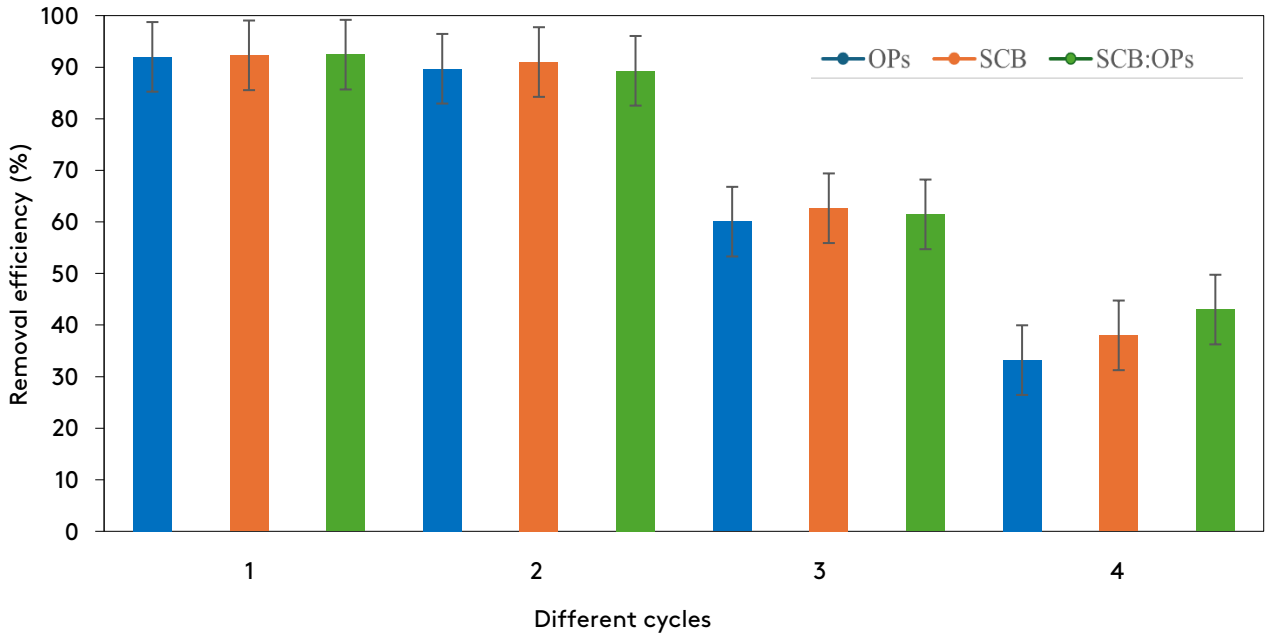

Fig. 12. Mn(II) adsorption-desorption cycles.

Figure 12 demonstrates the capacity for reusing bio-sorbents in the third and fourth cycles. The third cycle exhibited a minor decline in the percentage of substance removal for both bio-sorbents; the fourth cycle displayed the most significant reduction in adsorption capacity, with a percentage removal slightly above 30%. As the number of regeneration cycles increased, the mass of the bio-sorbents decreased, which explains the limited removal observed in the fourth cycle. Overall, these bio-sorbents could be effectively reused up to three times with satisfactory RE.

Studies have shown that the adsorption capacity of bio-sorbents decreases after each adsorption cycle. For instance, Yang et al. [38] used chitosan-encapsulated sargassum to remove Ni ions. They found that the bio-sorbent could be reused up to five times, but the mass loss of the bio-sorbent limited its reusability to the sixth cycle. The reusability of OPs was further justified by El Gheriany et al. [45], who used OPs for the sorption of oil spills in the Nile River. They found that OPs could be reused up to four times, with the fifth time showing significant mass loss and low RE. Therefore, when bio-sorbents such as SCB and OPs are used in water treatment, their little disposal may have negative effects on the environment. This challenge could be overcome through sorption-desorption processes, and it is still a challenge for scientists to find ways in which this biomass can be reused as many times as possible, thereby reducing any possible environmental effects of the released sludge.

The reduced ability of the bio-sorbents to adsorb metal ions in successive adsorption-desorption cycles can be influenced by multiple factors. One such factor is the diminishing accessibility of functional groups on the bio-sorbents' surface during reuse. This decreasing accessibility is connected to the bio-sorbents turning hydrophobic over time, causing them to repel water [47]. Consequently, this alteration limits their capability to bind water-soluble PTEs. Another factor to consider is that the active positions on the surface of these bio-sorbents become fully saturated, indicating that they are already loaded with metal ions. These modifications occur at the adsorption sites of the bio-sorbents, even following the application of acid washing aimed at removing metal ions. Acid washing is a widely employed method for rejuvenating bio-sorbents after the adsorption process. However, it fails to restore the bio-sorbents to their initial state fully. In addition, acid washing alters the structure of the bio-sorbent, consequently affecting its adsorption capacity as well [1].

3.9. Determination of Mn(II) by FAAS

The calibration curve for analysing Mn(II) in FAAS is shown in Figure 13.

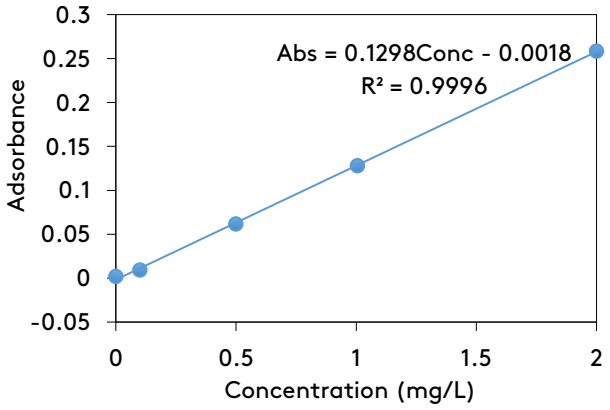

Fig. 13. Calibration curve for Mn(II) determination by FAAS.

The Beer-Lambert law stipulates that the concentration of a given compound in solution is directly proportional to the absorbance. Since the concentration and absorbance of a solution have a linear relationship, the concentration of a solution can be determined by observing its absorbance, which is the principle that FAAS is based on [48]. To determine the concentration of Mn using FAAS, the calibration curve was made for each set of measurements using a blank and four standards. Since all experiments were run in triplicate, the mean value was considered. However, this was not carried out if the coefficient of determination (R^2) was less than 0.999.

3.10. Limit of detection (LOD) and Limit of quantification (LOQ)

The LOD and LOQ for removing Mn(II) in simulated aqueous solutions using FAAS compared with values obtained from literature are recorded in Table 1.

Table 1. LOD and LOQ for Mn(II) determination.

Parameter	Experimental (mg/L)	Literature	Ref.
LOD	0.0099	0.0486	[49]
LOQ	0.0331	0.0616	[50]

These results were compared to the literature values reported by Forero-Mendieta et al. [49]. The values obtained in this study were lower than the reported values; these differences can be attributed to interference management techniques used, methodology settings, and the purity of the reagents [48].

3.11. Linearity, Accuracy, and Precision

The R^2 values obtained in this study ranged from 0.9991 to 1. According to Araujo [50], the data is acceptable when the R^2 value is 1 or close to 1. Analysis with FAAS was stopped when the R^2 value was less than 0.999, and the standards were prepared again before analysis could resume. The %RSD values for this study ranged between 1% to more than 5%. If the %RSD was over 5%, the results were not considered reliable and invalidated. The method of spiking was used for method validation in this study. Therefore, the accuracy was determined by spiking the simulated and wastewater solutions. The samples were spiked at 1×LOQ with 0.033 mg/L, and a percentage recovery of 77.95% was obtained. Spiking was also done at 10×LOQ with 0.331 mg/L, and a percentage recovery of 100.45% was obtained. These percentage recoveries are quantitative and confirm the accuracy of the Mn quantification method using FAAS. Furthermore, the spiking of wastewater samples enabled the confirmation of the method's accuracy in the real sample matrix.

4. Limitation of the study

Bio-sorbents, specifically SCB and OPs, are cost-effective and readily available adsorbents. As such, they are seen as alternative materials to conventional adsorbents since they are still under investigation, as confirmed by published articles. This is despite the use of various biomass materials, such as agricultural by-products (SCB and OPs), for PTE removal from aqueous solution. However, their usage is limited by various factors, including the loss of efficiency over time, the disposal of used bio-sorbents, and the desorption of pollutants may not be successful. Like other bio-sorbents, SCB and OPs are sensitive to operational conditions such as pH, ionic strength, and the presence of organic or inorganic ligands. In addition, they lack specificity in metal binding, while a large amount of biomass material is required to treat recalcitrant wastewater such as AMD.

5. Conclusions

Successful evaluation and comparison of the efficacy of individual and combined SCB and OPS for removing Mn(II) ions in simulated aqueous samples were performed. The effects of different parameters, including pH, contact period, bio-sorbent amount, and initial metal ion concentration on the adsorption of Mn(II), were investigated in adsorption studies. Pure and water-reacted bio-sorbents were characterized using different state-of-the-art characterization techniques to underpin the fate of Mn(II) post-adsorption, and useful information was drawn. The potential of OPs and SCB in Mn(II) removal from synthetic contaminated water was evaluated individually and compared. The findings further revealed that pH values and adsorbent dosage played a huge role in Mn(II) removal, while the contact time had little effect on Mn(II) attenuation for both OPs and SCB. In this study, the increase in bio-sorbent dosage led to a change in the color of the water, thereby, calling for the use of activated forms of bio-sorbent to limit possible environmental and health effects. Overall, the results revealed that the RE of OPs was greater than the RE of SCB because OPs gave results with the highest percentage removal of Mn(II) for all optimization parameters. This was highlighted by the SEM-EDS of the OPs after contact with water, which showed that OPs contained over 3% of Mn(II) while SCB had less than 1% of Mn(II). The homogenized SCB:OPs showed similar adsorption capacities to the individual bio-sorbents, which means they can be used interchangeably when one is not available due to seasonal variations. The bio-sorbents also showed good capacities towards the attenuation of Mn(II) in the presence of competitor ions. The bio-sorbents could also be reused over three times, showing their sustainability in water and wastewater treatment. The project will open the route to the concept of a circular economy approach (CEA) since agricultural by-products will be used to treat PTEs contaminated wastewater, thereby, controlling the environment and ensuring sustainable development for present and future generations.

Funding

Mr. Vincent Masilela received financial support from the National Research Foundation (NRF), grant number PMDS22070330879. This study was funded by the Water Research Commission (WRC) of South Africa, Project Number C2022/2023-00933.

Acknowledgements

The authors acknowledge the University of Johannesburg Research Centre for Synthesis and Catalysis and Spectrum for the facility.

References

[1] Varma, A.K., Mondal, P. (2016). Physicochemical Characterization and Pyrolysis Kinetic Study of Sugarcane Bagasse Using Thermogravimetric Analysis. Journal of Energy Resources Technology, Transactions of the ASME, 138(5), 1–11. https://doi.org/10.1115/1.4032729

[2] Kasim, N., Mohammad, A.W., Abdullah, S.R.S. (2016). Performance of membrane filtration in the removal of iron and manganese from Malaysia's groundwater. Membrane Water Treatment, 7 (4), 227–296. https://doi.org/10.12989/mwt.2016.7.4.277.

[3] Matveeva, V.A., Alekseenko, A.V., Karthe, D., Puzanov, A.V. (2022). Manganese Pollution in Mining-Influenced Rivers and Lakes: Current State and Forecast under Climate Change in the Russian Arctic. Water (Switzerland), 14 (7), 1-22. https://doi.org/10.3390/w14071091

[4] Aruna, N. Bagotia, A., Sharma, K., Kumar, S. (2021). A review on modified sugarcane bagasse biosorbent for removal of dyes. Chemosphere, 268(01), 1-18. https://doi.org/10.1016/j.chemosphere.2020.129309

[5] Chowdhury, I.R., Chowdhury, S., Mazumder, M.AJ., Al-Ahmed, A. (2022). Removal of lead ions (Pb^{2+}) from water and wastewater: a review on the low-cost adsorbents. Applied Water Science, 12(8), 1–18. https://doi.org/10.1007/s13201-022-01703-6

[6] Kullar, S.S., Shao, K., Surette, C., Foucher, D., Mergler, D., Cormier, P., Bellinger, D.C., Barbeau, B., Sauvé, S., Bouchard, M.F. (2019).

A benchmark concentration analysis for manganese in drinking water and IQ deficits in children. Environment International, 130, 1-8. https://doi.org/10.1016/j.envint.2019.05.083

[7] Edokpayi, J. N., Odiyo, J.O., Olasoji, S.O. (2014). Assessment of Heavy Metal Contamination of Dzindi River, in Limpopo province, South Africa. International Journal of Natural Sciences Research, 2(10), 185–194. http://pakinsight.com/?ic=journal&journal=63

[8] Madilonga, R.T., Edokpayi, J. N., Volenzo, E.T., Durowoju, O.S., Odiyo, J.O. (2021). Water Quality Assessment and Evaluation of Human Health Risk in Mutangwi River, Limpopo Province, South Africa. International Journal of Environmental Research and Public Health, 18(13), 53-65. https://doi.org/10.3390/ijerph18136765

[9] Khaskheli, M.I., Memon, S.Q., Siyal, A.N., Khuhawar, M.Y. (2011). Use of orange peel waste for Arsenic remediation of drinking water. Waste Biomass Valorization, 2(4), 423–433. https://doi.org/10.1007/s12649-011-9081-7

[10] Edokpayi, J., Rogawski, E., Kahler, D., Hill, C., Reynolds, C., Nyathi, E., Smith, J., Odiyo, J., Samie, A., Bessong, P., Dillingham, R. (2018). Challenges to sustainable safe drinking water: A case study of water quality and use across seasons in rural communities in Limpopo Province, South Africa. Water (Switzerland), 10(2), 159-170. https://doi:https://doi.org/10.3390/w10020159

[11] Addo-Bediako, A., Nukeri, S., Kekana, M. (2021). Heavy metal and metalloid contamination in the sediments of the Spekboom River, South Africa. Applied Water Science, 11(7), 1-9. https://doi.org/10.1007/s13201-021-01464-8

[12] Crafford, D., Luus-Powell, W., Avenant-Oldewage, A. (2014). Monogenean parasites from fishes of the Vaal Dam, Gauteng Province, South Africa II. New Locality Records, Acta Parasitologica, 59(3), 485-492. https://doi.org/10.2478/s11686-014-0271-x

[13] Soysüren, G., Yetgin, A.G., Arar, O., Arda, M. (2022). Removal of manganese(II) from aqueous solution by ionic liquid impregnated polymeric sorbent and electrodeionization (EDI) techniques. Process Safety and Environmental Protection, 158, 189–198. https://doi.org/10.1016/j.psep.2021.11.053

[14] Jin, H, Capareda, S. Chang, Z. Gao, Y. Xu, Zhang. J. (2014). Biochar pyrolytically produced from municipal solid wastes for aqueous As(V) removal: Adsorption property and its improvement with KOH activation. Bioresources and Technology, 169, 622–629. https://doi.org/10.1016/j.biortech.2014.06.103

[15] Hashtroudi, H., Farhadian, M., Borghei, M. (2023). Beet sugar wastewater treatment in a hybridbiological reactor: operational optimization and kinetic coefficients calculation. Advances in Environmental Technology, 9(4), 339–350. https://doi.org/10.22104/aet.2023.6325.1736

[16] Mahmudiono, T., Bokov, D., Widjaja, G., Konstantinov, I.S., Setiyawan, K., Abdelbasset, W.K., Madji, H.S., Kadhim, M.M., Kareem, H.A. Bansal, K. (2022). Removal of heavy metals using food industry waste as a cheap adsorbent. Food Science and Technology, 42, 1-6. https://doi.org/10.1590/fst.111721

[17] Afolabi, F.O., Musonge, P. Bakare, B.F. (2022). Adsorption of Copper and Lead Ions in a Binary System onto Orange Peels : Optimization Equilibrium and Kinetic Study. Sustainability, 14(17), 1-16. https://doi.org/10.3390/su141710860

[18] Molaudzi, N.R., Ambushe, A. A. (2022). Sugarcane Bagasse and Orange Peels as Low-Cost Biosorbents for the Removal of Lead Ions from Contaminated Water Samples. Water (Switzerland), 14(21), 1-25. https://doi.org/10.3390/w14213395

[19] Mohan, A. (2019). Study of Sugarcane Bagasse and Orange Peel as Adsorbent for Treatment of Industrial Effluent Contaminated with Nickel. International Research Journal of Engineering and Technology, 6(4), 4725–4731. https://www.irjet.net

[20] Qasem, N.A.A., Mohammed, R.H. Lawal, D.U. (2021). Removal of heavy metal ions from wastewater: a comprehensive and critical review. NPJ Clean Water, 4(1), 1–15. https://doi.org/10.1038/s41545-021-00127-0

[21] Mestek, O., Suchánek, M. Hrubý, V. (1999). Preparation and testing of standard solutions of cadmium, copper, and lead. Accreditation and Quality Assurance, 4(7), 307–312. https://doi.org/10.1007/s007690050372

[22] Öner, M., Demir, C., Çetin, G. Bakırdere, S. (2023). Development of a rapid and efficient analytical method for trace lead determination: Manganese dioxide nanoflower based dispersive solid-phase extraction. Journal of the International Measurement Confederation, 211, 1-7. https://doi.org/10.1016/j.measurement.2023.112606

[23] Nguegang, B., Masindi, V., Msagati, T.A.M. Tekere, M. (2021). The Treatment of Acid Mine Drainage Using Vertically Flowing Wetland: Insights into the Fate of Chemical Species. Minerals, 11(5), 1-24. https://doi.org/10.3390/min11050477

[24] Nguegang, B., Masindi, V., Msagati, T.A.M. Tekere, M. Mbue, N.I (2022). Assessing the performance of horizontally flowing subsurface wetland equipped with Vetiveria zizanioides for the treatment of acid mine drainage. Advance in Environmental Technology, 2, 123-127. https://doi.org/10.22104/AET.2022.5059.1370

[25] Ahmadi, A., Hafiz, S. S., Sharifi, H., Rene, N. N., Habibi, S. S., Hussain, S. (2022). Low cost biosorbent (Melon Peel) for effective removal of Cu (II), Cd (II), and Pb (II) ions from aqueous solution. Case Studies in Chemical and Environmental Engineering, 6, 1-7. https://doi.org/10.1016/j.cscee.2022.100242

[26] Akinhanmi, T.F., Ofudje, E.A., Adeogun, A.I., Aina, P. Joseph, I.M. (2020). Orange peel as low-cost adsorbent in the elimination of Cd(II) ion: kinetics, isotherm, thermodynamic and optimization evaluations. Bioresources and Bioprocessing, 7(1), 1-18. https://doi.org/10.1186/s40643-020-00320-y

[27] Rudi, N.N., Muhamad, M.S., Te Chuan, L., Alipal, J., Omar, S., Hamidon, N., Abdul Hamid, N.H., Mohamed Sunar, N., Ali, R., Harun, H. (2020). Evolution of adsorption process for manganese removal in water via agricultural waste adsorbents. Heliyon, 6(9), 1-13. https://doi.org/10.1016/j.heliyon.2020.e05049

[28] United States Environmental Protection Agency (USEPA). Drinking Water Health Advisory for Manganese. (2004). U.S. Environmental Protection Agency Office of Water, Washington, DC EPA-822-R-04-003, 1–49. https://doi.org/EPA-822-R-04-003

[29] Morais, L.C., Maia, A.A.D., Guandique, M.E.G., Rosa, A. H. (2017). Pyrolysis and combustion of sugarcane bagasse. Journal of Thermal Analysis and Calorimetry, 129(3), 1813–1822. https://doi:10.1007/s10973-017-6329-x

[30] Annadurai, G., Juang, R. S., Lee, D. J. (2018). Adsorption of Heavy Metals from Water Using Banana and Orange Peels. Water Science and Technology, 47(1), 185–190. https://doi.org/10.2166/wst.2003.0049

[31] Ali, A. (2017). Removal of Mn(II) from water using chemically modified banana peels as efficient adsorbent. Environmental Nanotechnology Monitoring Management, 7, 57–63. https://doi.org/10.1016/j.enmm.2016.12.004

[32] Rivas-Cantu, R.C., Jones, K. D., Mills, P. L. (2013). A citrus waste-based biorefinery as a source of renewable energy: Technical advances and analysis of engineering challenges. Waste Management and Research, 31(4), 413–420. https://doi:10.1177/0734242X13479432

[33] Afolabi, F.O., Musonge, P., Bakare, B.F. (2021). Application of the Response Surface Methodology in the Removal of Cu^{2+} and Pb^{2+} from Aqueous Solutions Using Orange Peels. Scientific African, 13, 1-11. https://doi.org/10.1016/j.sciaf.2021.e00931

[34] Mayerhöfer, T.G., Pipa, A.V., Popp, J. (2019). Beer's Law-Why Integrated Absorbance Depends Linearly on Concentration. Chemistry Physics, 20(21), 2748–2753. https://doi.org/10.1002/cphc.201900787

[35] Lemessa, G., Gabbiye, N., Alemayehu, E. (2023). Waste to resource: Utilization of waste bagasse as an alternative adsorbent to remove heavy metals from wastewaters in sub-Saharan Africa: A review. Water Practice and Technology, 18(2), 393–407. https://doi.org/10.2166/wpt.2023.011

[36] Narasingapillai, S., Sreenivasan, S. K. (2023). Adsorptive performance of sunflower seed ash as a novel biosorbent for the elimination of Congo red from aqueous solution. Advances in Environmental Technology, 9(4) 258–270. https://doi.org/10.22104/aet.2023.6131.1689

[37] Bade, M. M., Dubale, A. A., Bebizuh, D. F., Atlabachew, M. (2022). Highly Efficient Multisubstrate Agricultural Waste-Derived Activated Carbon for Enhanced CO_2 Capture. ACS Omega, 7(22), 18770–18779. https://doi.org/10.1021/acsomega.2c01528

[38] Yang, F., Liu, H., Qu, J., Chen, J.C. (2011). Preparation and characterization of chitosan encapsulated Sargassum sp. biosorbent for nickel ions sorption. Bioresource Technology, 102(3), 2821–2828. https://doi.org/10.1016/j.biortech.2010.10.038

[39] Masilela, V., Nguegang, B., Ambushe, A. A. (2023). Sugarcane Bagasse and Orange Peels as Potential Low-Cost Bio-Sorbents for Removal of Manganese(II) In Water. Universal Researchers, 54-60. https://doi.org/10.17758/iicbe4.c1122221

[40] Nguegang, B., Masindi, V., Msagati, T.A.M, Tekere, M. (2022). Effective treatment of acid mine drainage using a combination of MgO-nanoparticles and a series of constructed wetlands planted with Vetiveria zizanioides: A hybrid and stepwise approach. Journal of Environmental Management, 310, 114751. https://doi.org/10.1016/j.jenvman.2022.114751.

[41] Nguegang, B., Abayneh, A.A. (2024). Insight into the chemical and biochemical mechanisms governing inorganic contaminants removal by selective precipitation and neutralization in acid mine drainage treatment using MgO: A comparative study. Journal of Water Process Engineering, 59, 104924. https://doi.org/10.1016/j.jwpe.2024.104924.

[42] Lu, J.L., Chen, W. H. (2015). Investigation on the ignition and burnout temperatures of bamboo and sugarcane bagasse by thermogravimetric analysis. Applied Energy, 160, 49–57. https://doi:10.1016/j.apenergy.2015.09.026.

[43] Buthiyappan, A., Gopalan, J., Abdul, R.A.A. (2019). Synthesis of iron oxides impregnated green adsorbent from sugarcane bagasse: Characterization and evaluation of adsorption efficiency. Journal of Environmental Management. 249, 1–12. https://doi.org/10.1016/j.jenvman.2019.109323.

[44] Dey, S., Basha, S.R., Babu, G.V., Nagendra, T. (2021). Characteristic and biosorption capacities of orange peels bio-sorbents for removal of ammonia and nitrate from contaminated water. Cleaner Materials, 1, 1-24. https://doi.org/10.1016/j.clema.2021.100001

[45] El Gheriany, I.A., Ahmad El Saqa, F., Abd El Razek Amer, A., Hussein, M. (2020). Oil spill sorption capacity of raw and thermally modified orange peel waste. Alexandria Engineering Journal, 59(2), 925–932. https://doi.org/10.1016/j.aej.2020.03.024

[46] Wang, S., Shuang, Z., Zheng, X., Dao, X., Zheng, L., Yang, Y., Zhang, H., Binling, A., Sheng, Z. (2021). Calcite modification of agricultural waste biochar highly improves the adsorption of Cu(II) from aqueous solutions. Journal of Environmental Chemical Engineering, 9 (5), 106215. https://doi.org/10.1016/j.jece.2021.106215

[47] Nguegang, B., Abayneh, A.A. (2024). The treatment of acid mine drainage using a combination of selective precipitation and bio-sorption techniques: A hybrid and step-wise approach for AMD valorization and environmental pollution control. Environmental Research and Technology, 7(3), 313-334. https://doi.org10.35208/ert.1405067

[48] Pohl, P. (2020). A revisited FAAS method for very simple and fast determination of total concentrations of Cu, Fe, Mn and Zn in grape juices with sample preparation developed by modeling experimental design and optimization. Microchemical Journal, 157, 1–9. https://doi.org/10.1016/j.microc.2020.104998

[49] Forero-Mendieta, J.R., Varón-Calderón, J.D., Varela-Martínez, D.A., Riaño-Herrera, D.A., Acosta-Velásquez, R.D., Benavides-Piracón, J.A. (2022). Validation of an Analytical Method for the Determination of Manganese and Lead in Human Hair and Nails Using

Graphite Furnace Atomic Absorption Spectrometry. Separations, 9(7), 1-14. https://doi.org/10.3390/separations9070158

[50] Araujo, P. (2009). Key aspects of analytical method validation and linearity evaluation. Journal of Chromatography, 877, 2224–2234. https://doi.org10.1016/j.jchromb.2008.09.030

How to site this paper:

Masilela, V., Nguegang, B. & Ambushe, A. A. (2025). Investigating the removal of Mn(II) from water and wastewater using low-cost bio-sorbents: orange peels and sugarcane bagasse. Advances in Environmental Technology, 11(1), 13-35. DOI: 10.22104/aet.2024.6631.1814